

Enhanced Dichlorodifluoromethane Decomposition with Selective Fluorine Absorption by Acidic Fluorinated Magnesium Oxide

Tsukasa Tamai, Koji Inazu, and Ken-ichi Aika*

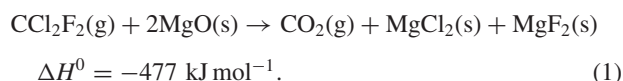
Department of Environmental Chemistry and Engineering, Interdisciplinary Graduate School of Science and Engineering, Tokyo Institute of Technology, 4259 Nagatsuta, Midori-ku, Yokohama 226-8502

Received October 2, 2003; E-mail: kenaika@chemenv.titech.ac.jp

CCl_2F_2 decomposition with simultaneous halogen absorption by partially fluorinated MgO (MgF_2 -MgO) was studied, focusing on the effects of the acidity of the surface. CCl_2F_2 decomposition by MgF_2 -MgO was greatly promoted by fluorination of MgO at 10 mol% or higher. CCl_2F_2 decomposition was not a catalytic process over MgF_2 -MgO but basically a selective fluorine absorption reaction with MgO to form MgF_2 . Chlorine was released in the form of CCl_4 regardless of reaction temperature and degree of fluorination of MgO due to low reactivity to CCl_4 . NH_3 -TPD and pyridine adsorption experiments were carried out to characterize the acid sites on MgF_2 -MgO samples. The amount of acid sites became maximum for 10% MgF_2 -MgO and the strength of acid sites increased as fluorination proceeded. CCl_2F_2 decomposition was revealed to be initiated by Lewis acid sites on MgF_2 -MgO formed by CCl_2F_2 decomposition as well as by fluorination with hydrofluoric acid aqueous solution. Thus, formation of the Lewis acid sites was considered to be the key step for efficient CCl_2F_2 decomposition with selective fluorine absorption.

Development of decomposition methods for chlorofluorocarbons (CFCs), which are one of major materials that deplete the stratospheric ozone layer, is an urgent issue. The catalytic hydrolysis of CFCs is a desirable method because it can be carried out under mild reaction conditions,^{1–8} but during the decomposition corrosive HCl and HF are formed and thus gas neutralizers and/or corrosion-proof systems are required. These often cause costly set-up or complicated operation in practical use. In most of the methods for CFC decomposition including catalytic processes, the reaction effluent is washed with NaOH aqueous solution and/or $\text{Ca}(\text{OH})_2$ to eliminate HF and HCl as halides.

Recently, for decomposition of halocarbons, direct fixation of halogens as metal halides, mainly alkaline metal and alkaline earth metal halides, have been reported. Destructive fixation of chlorocarbon and hydrochlorocarbon as metal chlorides has been well investigated. Weckhuysen et al. reported CCl_4 decomposition by La_2O_3 , CeO_2 , and various alkaline earth metal oxides^{9,10} and Klabunde and co-workers investigated destructive adsorption of CCl_4 by nano-scale structured MgO and CaO.^{11–16} They found that deposition of transition metal oxides to MgO and CaO promoted conversion of CCl_4 and adsorption capacity for chloride.^{11–14} However, for fluorine containing halocarbons such as CFCs and perfluorocarbons there have been just a few reports, including a report regarding CCl_2F_2 decomposition by sodium oxalate by Crabtree et al.^{17–19} We have focused on transition metal loaded MgO-based materials for CFC decomposition,²⁰ since MgO is inexpensive and available as material for uses such as catalyst support. Applying these materials to CCl_2F_2 , which was widely used as refrigerant, we found that addition of transition metal oxides to MgO to be quite effective; vanadium oxides especially were excellent additives that exhibit high conversion and selectivity to CO_2 and halides. In this system, the target reaction is as follows:



Supporting vanadium oxides on MgO enabled halogen absorption efficiency to be as high as ca. 80% when CCl_2F_2 was introduced in stoichiometric amounts to MgO at 723 K in a flow reaction system. Promotion of CCl_2F_2 decomposition by transition metal addition was considered to be related to the catalysis of supported transition metal oxides, i.e., the decomposition was initiated by the reaction of transition metal oxides with CCl_2F_2 to form transition metal halides. Most of these are unstable under the reaction conditions and readily react with MgO to generate transition metal oxides with magnesium halides as resulting products. However, this system also has a serious problem for practical use. In spite of their important role as intermediates, vanadium halides and/or oxyhalides will be deposited in the cooler part of the reactor due to their high volatility.

On the other hand, some research groups reported that acid sites on solid catalysts work as active sites for catalytic decomposition of CFCs^{6–8} and for dismutation or halogen exchange reaction for halocarbons.^{21–23} The acid sites can be generated by fluorination of the catalysts such as titanium dioxides,^{6,8} zeolites,⁷ and aluminium oxides^{21–23} by CFCs and HCFCs. Their effects were considered in connection with the induction period of the reaction. If the acid sites are introduced on MgO by such fluorination, high conversion of CFC can be expected. However, no study has been conducted on introducing acid sites to a basic oxide, MgO. In this study we have examined the effectiveness of fluorination of MgO to CCl_2F_2 decomposition by MgF_2 -MgO with simultaneous halogen fixation as magnesium halides. Fluorination of MgO by soaking in hydrogen fluoride aqueous solution was found to be an effective

method to generate acid sites on MgO as well as fluorination of MgO during CCl_2F_2 decomposition. Introducing such acid sites on MgO greatly enhanced the reaction of CCl_2F_2 with MgF_2 - MgO to form MgF_2 , CO_2 , and CCl_4 . The acid sites were characterized by NH_3 -TPD and pyridine adsorption experiments to reveal their relevance to CCl_2F_2 decomposition and halogen absorption by MgF_2 - MgO .

Experimental

Materials. MgO was prepared by following procedure: Commercial MgO powder (Ube Materials Industries) was suspended in deionized water and the suspension was stirred overnight at room temperature. After being dried, the resulting $\text{Mg}(\text{OH})_2$ was calcined at 873 K for 3 h under helium flow to form MgO with high surface area. Partially fluorinated MgO was prepared by adding HF to aqueous suspensions of MgO prepared by the method mentioned above, followed by drying procedure and calcination under the same conditions as those for MgO . The samples are denoted, for example, 10% MgF_2 - MgO for partially fluorinated MgO with the degree of fluorination at $\text{MgF}_2/(\text{MgF}_2 + \text{MgO}) = 0.1$ mol/mol.

CCl_2F_2 Decomposition. Reactions of CCl_2F_2 with MgO and partially fluorinated MgO were performed using a fixed-bed flow reactor system under atmospheric pressure. 1% CCl_2F_2 balanced with helium was fed to 0.2 g of the MgO samples placed in a tubular quartz reactor at a total flow rate of 30 mL/min after MgO samples were pretreated under helium flow at 873 K for 3 h. Analysis of outlet gas was carried out by using a GC-TCD (Shimadzu GC-14B) with a Porapak Q column to determine conversion of CCl_2F_2 and selectivity to carbon dioxide. Feeding a stoichiometric amount of CCl_2F_2 to the samples was attained at the reaction time of 3.3 h. When complete conversion of CFCs was achieved, MgO would be totally consumed to be MgCl_2 and MgF_2 during this period of time.

CCl_4 Decomposition. CCl_4 decomposition by the MgO sample was carried out using a fixed-bed pulse reaction system directly connected to GC-TCD. A pulse injection of CCl_4 (Wako, 99%) was made to the same reactor as that used for CCl_2F_2 decomposition system at 723 K with a precision syringe.

Characterization. X-ray diffraction patterns of the samples were obtained with Rigaku Multi-flex S with $\text{Cu K}\alpha$ radiation as an incident X-ray source in the range of 20 to 70 degrees as 2θ . The specific surface area of each sample was determined by nitrogen adsorption at 77 K with BELSORP 28SA (BEL Japan).

NH_3 -TPD experiments were carried out for MgO samples by using a Pyrex glass system equipped with a quartz U-tube reactor. The samples were pretreated at 873 K for 2 h under evacuation. After the sample was cooled down to 373 K, gaseous ammonia was introduced to the system and then adsorption equilibrium was attained within 30 min. Temperature programmed desorption of ammonia was performed at a temperature ranging from 373 to 873 K with detection by TCD (Shimadzu GC-8A) after removing physisorbed ammonia under vacuum for 0.5 h.

The FT-IR analysis for the MgO samples were performed in a quartz cell connected to a closed system made of Pyrex. A self-supported thin sample disc (ca. 0.1 g) was placed in the quartz IR cell and pretreated at 873 K for 2 h under vacuum. And then about 10 Torr of pyridine was introduced to the cell at room temperature to be adsorbed for 30 min, followed by evacuation at given temperatures for 1 h. IR spectra were taken with JASCO VALOR III under the following conditions: 32 repeated scans, resolution of 2 cm^{-1} ,

and MCT detection.

Results and Discussion

CCl_2F_2 Decomposition by Partially Fluorinated MgO .

As shown in Fig. 1(a), CCl_2F_2 did not substantially react with MgO at 623 K, however, CCl_2F_2 was decomposed to form CO_2 and CCl_4 as major gas-phase product by the reaction with the MgO samples partially fluorinated by dilute hydrofluoric acid aqueous solution (MgF_2 - MgO). Almost complete conversion of CCl_2F_2 was observed for all the MgF_2 - MgO samples that had 5% or higher fluorination by mole. For a sample to exhibit significant activity to CCl_2F_2 decomposition, 5% was a threshold value for the extent of fluorination of MgO . An induction period of about 1 h was also observed for the decomposition by MgF_2 - MgO except for 5% MgF_2 - MgO , which required 2.5 h to attain CCl_2F_2 conversion of more than 80%. There was a tendency for the induction period to be shortened with an increase in percentage fluorination of MgO . On the other hand, as shown in Fig. 1(b), the selectivity to CO_2 was almost constant at about 50% during the reaction time examined for the samples other than 5% MgF_2 - MgO , with which an induction period of 2.5 h was observed. The rest of the carbon from CCl_2F_2 was dominantly in the form of CCl_4 , an undesired product, as mentioned above, although a trace amount of CCl_3F was also observed as the reaction prolonged. The observed distribution of gas-phase product indicates that decomposition of

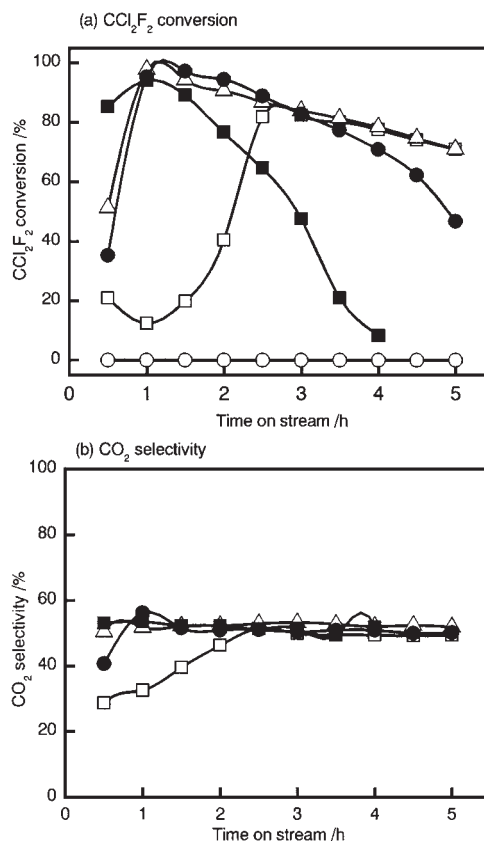


Fig. 1. Time course of CCl_2F_2 conversion (a) and CO_2 selectivity (b) in CCl_2F_2 decomposition at 623 K by partially fluorinated MgO . Percentage fluorination of MgO : 0% (○), 5% (□), 10% (△), 20% (●), 40% (■).

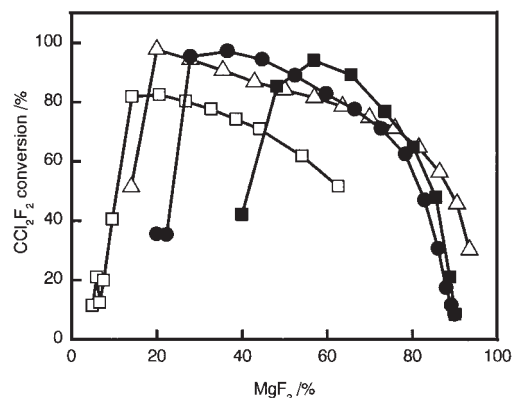
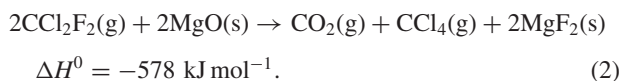


Fig. 2. Relationship between degree of fluorination and CCl_2F_2 conversion during CCl_2F_2 decomposition for partially fluorinated MgO with different initial percentage fluorination at 623 K. Percentage fluorination of MgO: 5% (\square), 10% (\triangle), 20% (\bullet), 40% (\blacksquare).

CCl_2F_2 by MgF_2 -MgO samples takes place with the following reaction (Eq. 2):



Along with the reaction of Eq. 2, fluorine of CCl_2F_2 is fixed in the solid phase exclusively as MgF_2 . It means that the decomposition of CCl_2F_2 by MgF_2 -MgO is accompanied by selective fluorine absorption to yield MgF_2 as the only solid phase product. As decomposition of CCl_2F_2 proceeded nearly according to Eq. 2, the conversion of MgO can be calculated from the yield of CO_2 in this system. Figure 2 shows the dependence of CCl_2F_2 conversion upon the mole percentage of MgF_2 in MgF_2 -MgO for each sample. Initially, CCl_2F_2 conversion increased with an increase in mole percentage of MgF_2 in MgF_2 -MgO. When the mole percentage of MgF_2 became 80% or higher, CCl_2F_2 conversion steeply decreased and the decomposition will be terminated at around 90%. This suggests that the induction period observed at the initial stage of the decomposition is the period to attain a certain concentration level of MgF_2 needed to exhibit high reactivity to CCl_2F_2 .

Since reaction temperature should be an important factor affecting the decomposition and product distribution, temperature dependence of CCl_2F_2 conversion and CO_2 selectivity was investigated for 10% MgF_2 -MgO. Results are shown in Fig. 3(a) and (b), respectively. At 573 K, CCl_2F_2 conversion was quite low. Therefore the result of CO_2 selectivity at this temperature was omitted due to the low and inaccurately measured yield.

Reactions at temperatures above 623 K gave almost complete CCl_2F_2 conversion at the reaction time of 2 h and stable CO_2 formation with the selectivity of ca. 50%. At reaction temperatures above 673 K, no induction period for CCl_2F_2 conversion was observed without any changes in CO_2 selectivity. It indicates that the decomposition at 623 K or higher temperatures proceeds along with the same pathway. Temperature dependence of the reaction of CCl_2F_2 with MgO was also examined for comparison with MgF_2 -MgO samples and the result is shown in Fig. 4. When the reaction temperature became 773 K, conversion of CCl_2F_2 started after the induction period of 2.5 h.

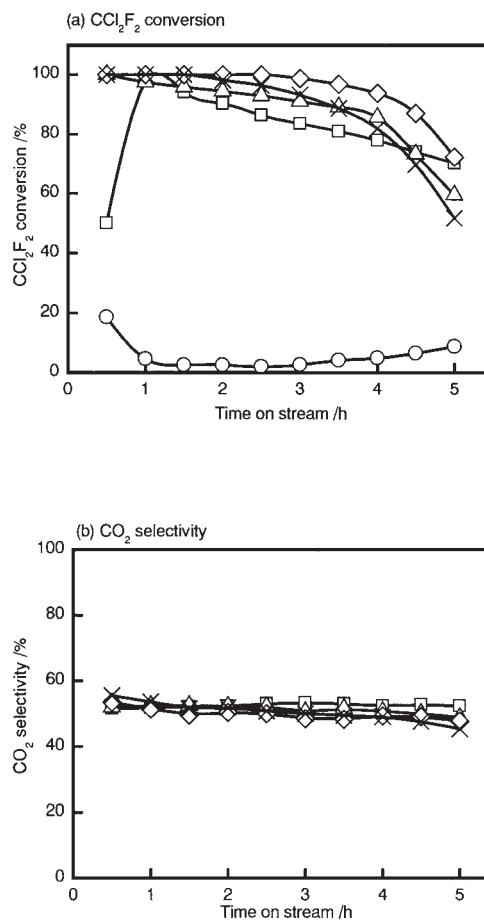


Fig. 3. Temperature dependence of CCl_2F_2 conversion (a) and CO_2 selectivity (b) in CCl_2F_2 decomposition by 10% MgF_2 -MgO. Reaction temperature: 573 K (\circ), 623 K (\square), 673 K (\triangle), 723 K (\diamond), 773 K (\times).

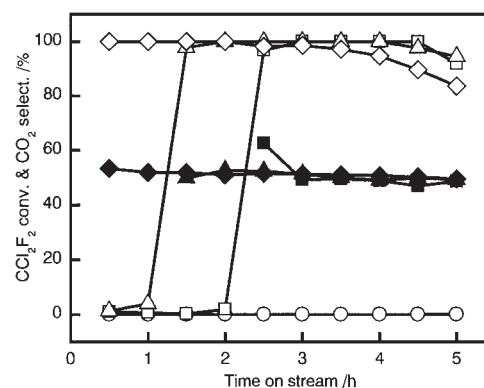


Fig. 4. Temperature dependence of CCl_2F_2 decomposition by MgO. Reaction temperature: 723 K (\circ), 773 K (\square), 823 K (\triangle), 873 K (\diamond). CCl_2F_2 conversion (open), CO_2 selectivity (close).

The induction period decreased to 1.5 h at 823 K, which is comparable to that for MgF_2 -MgO at 623 K. Although the reproducibility of the induction period was not excellent probably due to slight differences in the preparation conditions of the samples, higher reaction temperatures definitely showed shorter induction periods and conversion of CCl_2F_2 reached 100% after

the induction period. Once the conversion occurred, no significant differences in stability of gas-phase product distribution, CCl_2F_2 conversion, and CO_2 selectivity were observed. These observations indicate that MgO requires a temperature higher by 150–200 K than MgF_2 - MgO does to be capable to decompose CCl_2F_2 and that MgO can be activated by partial fluorination by the reaction with CCl_2F_2 in the same manner as fluorination by hydrofluoric acid. It is also confirmed by these observations that partial fluorination of MgO greatly enhances the decomposition of CCl_2F_2 with selective fluorine absorption.

XRD Analysis and NH_3 -TPD Measurement. As described above, partial fluorination of MgO using hydrofluoric acid formed highly reactive MgF_2 - MgO to CCl_2F_2 decomposition with selective fluorine absorption. Results also suggested that MgF_2 - MgO can be produced by the reaction with CCl_2F_2 at temperatures above 623 K. To confirm the chemical composition of MgF_2 - MgO samples prepared with dilute hydrofluoric acid aqueous solution, we performed X-ray diffraction (XRD) analysis for five kinds of MgF_2 - MgO with different degrees of fluorination, as well as MgO and MgF_2 (Fig. 5). As easily expected, diffraction peaks that originated from MgF_2 were detected for most of the MgF_2 - MgO samples. Although the fluorination at 5% and 10% significantly modified the base MgO , as seen in the activity to CCl_2F_2 decomposition, the diffraction peaks from MgF_2 were detected only for the samples with the degrees of fluorination of 20% or higher. This limitation should be either due to lack of sufficient sensitivity with XRD or due to very small particle sizes of MgF_2 crystallites in 5% and 10% MgF_2 - MgO samples.

As shown in Table 1, the particle size of MgO , which was calculated from full width at half height (FWHM) of a diffraction peak at 2θ of 42.9° that originated from the (200) facet, became slightly smaller as MgO became highly fluorinated. As reported by Shimbo et al., covering MgO particles with hydrofluoric acid can prevent the particles from sintering during heat

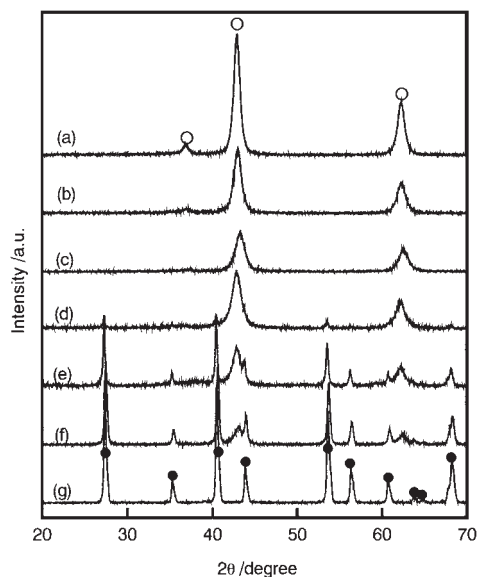


Fig. 5. XRD patterns of partially fluorinated MgO . Percentage fluorination of MgO : 0% (MgO) (a), 5% (b), 10% (c), 20% (d), 40% (e), 70% (f), 100% (MgF_2) (g). MgO (○), MgF_2 (●).

Table 1. Particle Size of MgO and MgF_2 in Partially Fluorinated MgO

Percentage fluorination	Particle size/nm	
	$\text{MgO}^{\text{a)}$	$\text{MgF}_2^{\text{b)}$
0 ^{c)}	8.8	n.d. ^{d)}
5	8.6	n.d. ^{d)}
10	7.5	n.d. ^{d)}
20	7.0	27
40	n.d. ^{d)}	29
70	n.d. ^{d)}	25
100 ^{e)}	n.d. ^{d)}	28

a) Determined by XRD peak of MgO (200) at $2\theta = 42.9^\circ$ degree. b) Determined by XRD peak of MgF_2 (110) at $2\theta = 27.3^\circ$ degree. c) Conventionally prepared MgO . d) Not determined because of low peak intensity or overlap of another peak. e) Commercial MgF_2 .

Table 2. BET Surface Area and Results of NH_3 -TPD for Partially Fluorinated MgO

Percentage fluorination	BET surface area/ $\text{m}^2 \text{g}^{-1}$	NH_3 -adsorbed ^{a)}	
		$\mu\text{mol g}^{-1}$	$\mu\text{mol m}^{-2}$
0	192	18	0.09
5	179	86	0.48
10	233	153	0.66
20	187	146	0.78
40	127	127	1.00
70	58	76	1.31
100	<1	trace	—

a) Adsorbed at 373 K, desorbed from 373 to 873 K.

treatment and hence core MgO in MgF_2 - MgO particles can keep their size as small as they were originally even after treatment at 873 K.²⁴ On the other hand, for MgF_2 in MgF_2 - MgO , the difference in degree of fluorination caused no clear tendency for changes in the particle size, which was calculated from FWHM of a peak at 2θ of 27.3° that originated from the (110) facet. The particle sizes of MgF_2 of MgF_2 - MgO samples, ranging from 25 to 30 nm, were coincidentally similar to that of commercial MgF_2 (28 nm).

NH_3 -TPD was carried out to estimate the amount and the strength of acid sites on MgF_2 - MgO samples. The results of BET surface area and NH_3 -TPD measurement are listed in Table 2 and the NH_3 -TPD profiles are shown in Fig. 6. The largest BET surface area of MgF_2 - MgO samples was obtained with 10% MgF_2 - MgO ($233 \text{ m}^2 \text{g}^{-1}$) and the degree of fluorination higher than 10% gave smaller surface area. Low specific surface area of MgF_2 can account for this tendency, even though the particle size of MgO was kept small during the fluorination in a similar manner to the case described above. The amount of adsorbed ammonia increased drastically with an increase in degree of fluorination up to 10%. 10% MgF_2 - MgO had the largest amount of adsorbed ammonia of $153 \mu\text{mol g}^{-1}$. Higher degree of fluorination than 10% gave smaller amount of adsorbed ammonia, however, surface density of acid sites, i.e., specific amount of adsorbed ammonia by surface area, increased with an increase in the degree of fluorination. Commercial MgF_2 had quite small surface area and no meaningful amount of NH_3 adsorption.

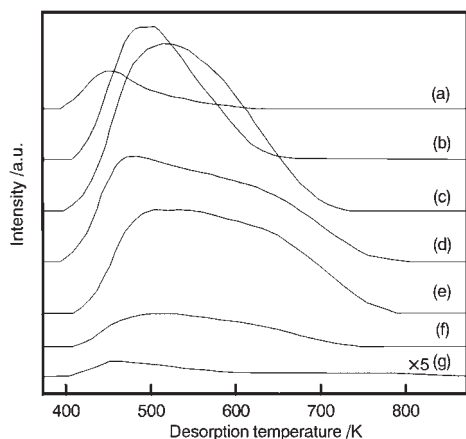


Fig. 6. NH_3 -TPD profiles of partially fluorinated MgO. Percentage fluorination of MgO: 0% (MgO) (a), 5% (b), 10% (c), 20% (d), 40% (e), 70% (f), 100% (MgF_2) (g).

The NH_3 -TPD profiles shown in Fig. 6 indicate that desorption temperature of NH_3 shifted to higher as fluorination proceeded, and from 20% of fluorination a broad peak that spread from 450 to 750 K was observed. It clearly indicates that there were acid sites with different strength on MgF_2 -MgO, and that the strength of acid sites increased by partial fluorination of MgO as well as the number of acid sites. Commercial MgF_2 has desorption peaks at 450 K, which shows weak acidity.

IR Observation of Pyridine Adsorption. Pyridine has been used as a typical probe adsorbate molecule to characterize surface acidity. It has also been found that pyridine interacts with ionic metal oxides in three different modes. The first mode corresponds to transfer of a proton from surface hydroxy group to form a pyridinium ion (Brønsted, BPy). The second one corresponds to coordination of the lone pair of nitrogen atom with a Lewis acid site such as some metal ion (LPy bonding mode). The last one, the weakest interaction among the three, is made through hydrogen bonding of pyridine to surface OH groups. Since MgO is a basic oxide, there have been quite a few reports dealing with the acidity of MgO.^{25,26} According to the above NH_3 -TPD results, acid sites on MgF_2 -MgO samples were considered to be generated by fluorination of MgO. To characterize the acid sites, we carried out pyridine adsorption experiments for partially fluorinated MgO by means of FT-IR. Before pyridine was introduced onto the samples, each sample was pretreated under vacuum at 873 K for 2 h and then cooled down to room temperature. The IR spectrum after pretreatment was used as background spectrum for pyridine adsorption experiments for each sample. Pyridine was introduced onto the samples for 30 min at ambient temperature and then evacuated at elevated temperatures from 298 to 573 K. The spectra obtained are shown in Fig. 7 for MgO (a), 10% MgF_2 -MgO (b), and 40% MgF_2 -MgO (c). In the range from 1400 to 1630 cm^{-1} , four distinct peaks were observed at 1440–1451, 1480–1496, 1570–1580, and 1595–1615 cm^{-1} . These peaks originate from the ring vibration mode of pyridine assigned to 19b, 18a, 8b, and 8a modes by Kline and Turkevich.²⁷ 19b and 8a modes are often used to distinguish between LPy mode, physisorbed, and BPy. Physisorbed or hydrogen-bonded pyridine gave the bands at 1440–1445 cm^{-1} (19b) and 1580–1600 cm^{-1} (8a), while pyridine in LPy mode gave the bands at 1445–1460 cm^{-1} (19b)

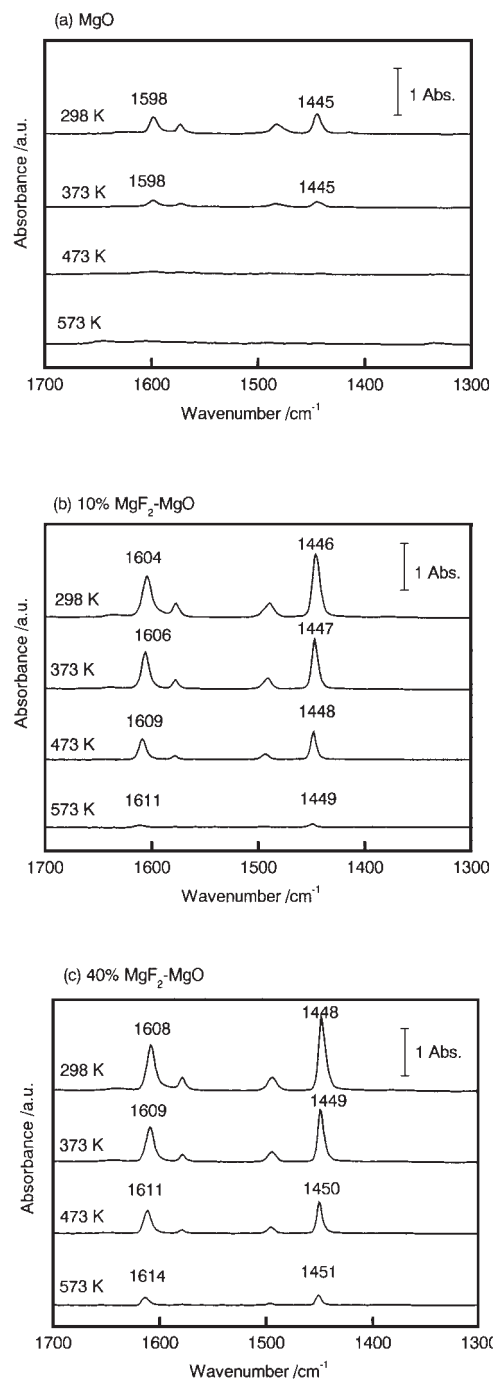


Fig. 7. IR spectra of pyridine adsorbed on MgO (a), 10% MgF_2 -MgO (b), and 40% MgF_2 -MgO (c) at desorption temperatures ranging from 298 to 573 K.

and 1602–1634 cm^{-1} (8a). BPy mode gives the bands at 1540 cm^{-1} and 1640 cm^{-1} .²⁸ After evacuation at room temperature, pyridine on MgO shows distinct adsorption bands of 19b and 8a at 1445 cm^{-1} and 1598 cm^{-1} , respectively. However, the peaks from excess and weakly adsorbed pyridine became smaller by evacuation at higher temperatures and they disappeared at 473 K. This observation indicates that adsorption of pyridine on MgO is a weak physical adsorption and thus the peaks at 1445 cm^{-1} (19b) and 1598 cm^{-1} (8a) can be assigned as originating from physically adsorbed pyridine or as adsorbed

on very weak Lewis acid sites, which can remain on the surface under vacuum at temperatures below 473 K.

10% $\text{MgF}_2\text{-MgO}$ and 40% $\text{MgF}_2\text{-MgO}$ were used as representative $\text{MgF}_2\text{-MgO}$ samples, since they showed distinct differences in the length of induction period in CCl_2F_2 decomposition at 623 K (Fig. 1) and $\text{NH}_3\text{-TPD}$ profile (Fig. 6). Based on the wavenumber of the peaks from 19b and 8a modes, pyridines on both samples were assigned to be adsorbed at Lewis acid sites. However, a small amount of physically adsorbed pyridine was also included at 298 K, and 373 K for both samples. The intensity of all four peaks decreased and the wavenumbers of the peaks from 19b and 8a modes slightly shifted to higher values as evacuation temperature rose. For example pyridine adsorbed on 40% $\text{MgF}_2\text{-MgO}$ showed the peaks at 1448 cm^{-1} (19b) and 1608 cm^{-1} (8a) at 298 K, while at 573 K this value shifted to 1451 cm^{-1} (19b) and 1614 cm^{-1} (8a). This fact indicates that $\text{MgF}_2\text{-MgO}$ samples have Lewis acid sites that are different in strength. Stronger Lewis acid sites, from which pyridine did not desorb at higher evacuation temperature, have been reported to show the peaks at higher wavenumber as 19b^{29,30} and 8a modes.²¹ Since the geometry of adsorbed pyridine is almost the same for all the samples used, Lewis acidity of acid sites on $\text{MgF}_2\text{-MgO}$ samples can be compared by the wavenumber of the peaks from 19b and 8a modes. Pyridine on 40% $\text{MgF}_2\text{-MgO}$ showed wavenumbers of the peaks from 19b and 8a modes higher than those on 10% $\text{MgF}_2\text{-MgO}$ at any temperature employed; for example, at the evacuation temperature of 573 K, the wavenumber of the peaks were 1451 cm^{-1} (19b) and 1614 cm^{-1} (8a) for 40% $\text{MgF}_2\text{-MgO}$, while they were 1449 cm^{-1} (19b) and 1611 cm^{-1} (8a) for 10% $\text{MgF}_2\text{-MgO}$. The peaks remaining at 573 K, which originated from stronger Lewis acid sites, were more intense for 40% $\text{MgF}_2\text{-MgO}$ than for 10% $\text{MgF}_2\text{-MgO}$. This fact indicates that 40% $\text{MgF}_2\text{-MgO}$ has more and stronger acid sites than 10% $\text{MgF}_2\text{-MgO}$. 20% $\text{MgF}_2\text{-MgO}$ gave almost the same results as for 40% $\text{MgF}_2\text{-MgO}$, although the results are not shown here. This indicates that the degree of fluorination over 20% can give sufficient Lewis acid sites in both number and strength. No spectrum obtained in this study showed any bands at 1540 cm^{-1} and 1640 cm^{-1} from Brønsted acid sites. The feasibility of observation of Brønsted acid sites on MgO by pyridine adsorption is still obscure, because previously reported results have some discrepancies: Itoh et al. reported that pyridine did not interact with Brønsted acid sites on MgO,²⁵ while López and Gómez reported the observation of PyB modes on MgO prepared by a sol-gel method hydrolyzed with hydrochloric acid.²⁶ In our partially fluorinated MgO samples, it might be possible that trace amounts of residual hydroxy groups which remain after thermal treatment at 873 K have Brønsted acid sites, which are not detectable by infrared spectroscopy using pyridine as probe molecule. Nevertheless, such Brønsted acid sites cannot be so important since there is no water and hydrogen source to generate Brønsted acid sites in the system employed in this study, while Brønsted acidity is an important factor in hydrolysis of CCl_2F_2 over solid catalysts where abundant water vapor exists in the system.

Changes of 5% $\text{MgF}_2\text{-MgO}$ during CCl_2F_2 Decomposition. The results shown above reveal that the reactivity to CCl_2F_2 , acid characteristics, and the morphology of MgO are

changed by partial fluorination to form $\text{MgF}_2\text{-MgO}$. MgO was also fluorinated during CCl_2F_2 decomposition, and 5% $\text{MgF}_2\text{-MgO}$ was employed as a typical $\text{MgF}_2\text{-MgO}$ sample to observe the fluorination of MgO by the reaction with CCl_2F_2 . The time dependences of CCl_2F_2 conversion and products yield for 5% $\text{MgF}_2\text{-MgO}$ at 723 K are shown in Fig. 8. Since CCl_2F_2 decomposition by $\text{MgF}_2\text{-MgO}$ is exclusively selective fluorine absorption with formation of CO_2 and CCl_4 described above as Eq. 2, the fluorination degree of MgO can be calculated based on the yields of CO_2 at corresponding reaction times. As described above, there was an induction period for CCl_2F_2 conversion, probably due to active acid site generation by the reaction. The degree of MgO fluorination simply increased with an increase in reaction time although the rate of the increase got smaller when the fluorination degree approached 90%.

The result of XRD analysis at different reaction times is shown in Fig. 9. The intensity of the diffraction peaks from MgO and the corresponding increase in the peaks from MgF_2 were observed with an increase of reaction time. No substantial diffraction peak from MgCl_2 was observed for all the samples.

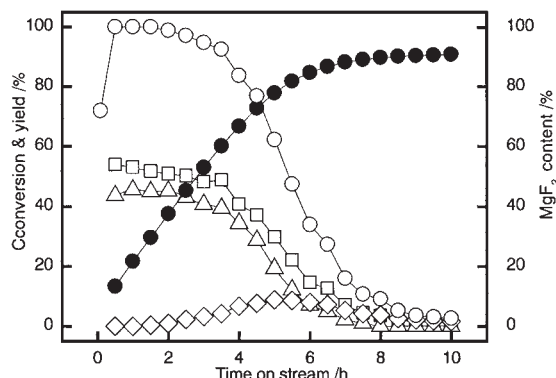


Fig. 8. Time course of CCl_2F_2 decomposition by 5% $\text{MgF}_2\text{-MgO}$ at 723 K. CCl_2F_2 conversion (\circ), CO_2 yield (\square), CCl_4 yield (\triangle), CCl_3F yield (\diamond), ratio of MgF_2 in the sample (\bullet).

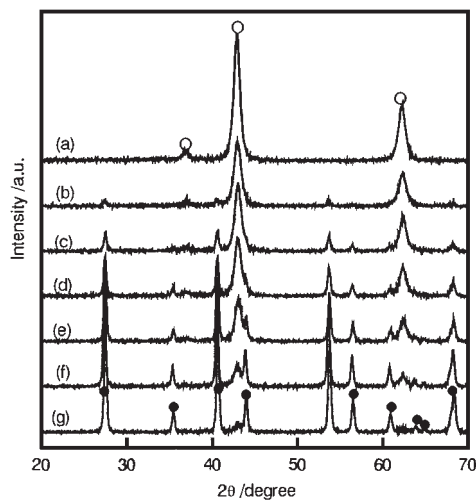


Fig. 9. XRD patterns of 5% $\text{MgF}_2\text{-MgO}$ during CCl_2F_2 decomposition at 723 K. Reaction time: 0 h (a), 0.5 h (b), 1 h (c), 2 h (d), 3 h (e), 5 h (f), 10 h (g). MgO (\circ), MgF_2 (\bullet).

Table 3. Changes in Particle Size of MgO and MgF₂ in 5% MgF₂-MgO during CCl₂F₂ Decomposition

Reaction time /h	Particle size/nm	
	MgO ^{a)}	MgF ₂ ^{b)}
0	8.6	n.d. ^{c)}
0.5	9.5	n.d. ^{c)}
1	9.5	22
2	n.d. ^{c)}	23
3	n.d. ^{c)}	24
5	n.d. ^{c)}	26
10	n.d. ^{c)}	26

Reaction condition: 1% CCl₂F₂, 723 K, 0.2 g of 5% MgF₂-MgO. a) Determined by XRD peak of MgO (200) at 2θ = 42.9 degree. b) Determined by XRD peak of MgF₂ (110) at 2θ = 27.3 degree. c) Not determined because of low peak intensity or overlap of another peak.

Table 4. BET Surface Area and Results of NH₃-TPD for 5% MgF₂-MgO during CCl₂F₂ Decomposition

Reaction time /h	Surface area /m ² g ⁻¹	NH ₃ -adsorbed ^{a)}	
		μmol g ⁻¹	μmol m ⁻²
0	179	86	0.48
0.5	137	141	1.03
1	113	140	1.24
2	78	95	1.22
3	58	78	1.35
5	31	56	1.79
10	15	39	2.52

Reaction condition: 1% CCl₂F₂, 723 K, 0.2 g of 5% MgF₂-MgO. a) Adsorbed at 373 K, desorbed from 373 to 873 K.

These observations agree with the result of gas-phase product analysis and Eq. 2. The crystallite size of MgO was almost constant at 8 to 9 nm, as shown in Table 3, while the size of MgF₂ slightly increased from 22 to 26 nm after the reaction for 5 h. This result indicates that a part of MgO is once fluorinated by the reaction with CCl₂F₂ to have a higher degree of fluorination, then fluorine absorption in CCl₂F₂ decomposition proceeds dominantly on the MgF₂-MgO with higher degree of fluorination until MgO in the MgF₂-MgO is almost completely consumed to be MgF₂, then another MgF₂-MgO with low or initial degree of fluorination starts to react with CCl₂F₂. In other words, CCl₂F₂ decomposition with fluorine absorption proceeds sequentially from the top layer at upstream to bottom part in downstream.

BET surface area and the amount of adsorbed ammonia on MgF₂-MgO after different periods of reaction are listed in Table 4. The surface area of MgF₂-MgO monotonously decreased as the reaction proceeded. The amount of adsorbed ammonia, i.e., the number of acid sites, increased until 0.5 h, at which initially employed 5% MgF₂-MgO changed to 13% MgF₂-MgO (Fig. 8) and a broad desorption peak of ammonia from 450 to 750 K started to develop in NH₃-TPD (Fig. 10). This result is consistent with that for partially fluorinated MgO prepared with HF, for example, 10% MgF₂-MgO had the largest number of acid sites and a broad desorption peak in NH₃-TPD. In this way, characteristics of acid sites on

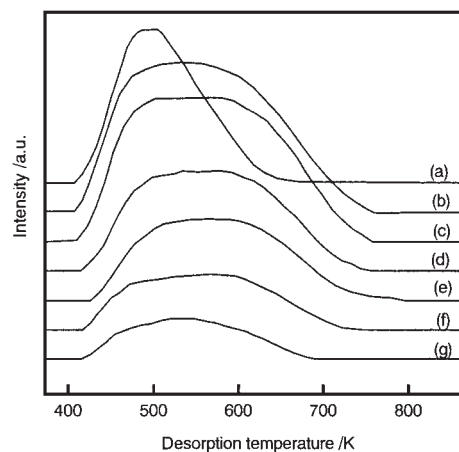


Fig. 10. NH₃-TPD profiles of 5% MgF₂-MgO during CCl₂F₂ decomposition. Reaction time: 0 h (a), 0.5 h (b), 1 h (c), 2 h (d), 3 h (e), 5 h (f), 10 h (g).

MgF₂-MgO are almost independent of the method of fluorination of MgO but are dependent on the degree of fluorination. However, it would be also true that some characteristics of the acid sites are different for the MgF₂-MgO samples prepared by these two different methods, because a little amount of chlorine could be adsorbed on MgF₂-MgO formed by CCl₂F₂ decomposition and lateral distribution of acid sites should be different, which may affect the characteristics of acid sites.

Generation of Acid Sites by Fluorination. The above results revealed that Lewis acid sites were formed by fluorination of both HF and CCl₂F₂. Commercial MgF₂ had quite small surface area and poor acidity (Table 2), and crystalline MgF₂ in partially fluorinated MgO was similar to commercial MgF₂ as judged from particle size of MgF₂ (Tables 1 and 3). Thus, generated acidity is not derived from MgF₂, but is derived from the interface of MgF₂ and MgO. The acidity of MgF₂ is reported to be weak, which is inactive to disproportionation reactions of chlorofluorocarbons.³¹⁻³³ As described in the introduction, there are many reports about fluorination of metal oxide and effects of fluorination, although there is no report about fluorination of MgO. The reason for increase in acidity of metal oxides by fluorination is briefly explained as follows. Partial replacement of surface oxygen and/or hydroxy groups by more electronegative fluorine increased the polarity of the metal oxide lattice, making the nearby Brønsted and Lewis acid sites more acidic.⁶

Role of Acid Sites on MgF₂-MgO in Total Decomposition of CCl₂F₂. Partially fluorinated MgO effectively decomposed CCl₂F₂ to CO₂ and CCl₄ with fluorine absorption as MgF₂, while the desirable reaction is the total decomposition to CO₂ and solid halides. If CCl₄ is completely decomposed with chlorine fixation as MgCl₂, total decomposition of CCl₂F₂ with simultaneous absorption of both chlorine and fluorine is attained. The reason why selective fluorine absorption exclusively takes place should be related to the reactivity of MgF₂-MgO to CCl₄. In order to confirm this, we performed CCl₄ decomposition experiments by MgO and partially fluorinated MgO using a pulse-reaction system. Results are shown in Fig. 11. Regardless of the degree of fluorination, in other words independent of the acidity of the sample, prompt deactivation within a few

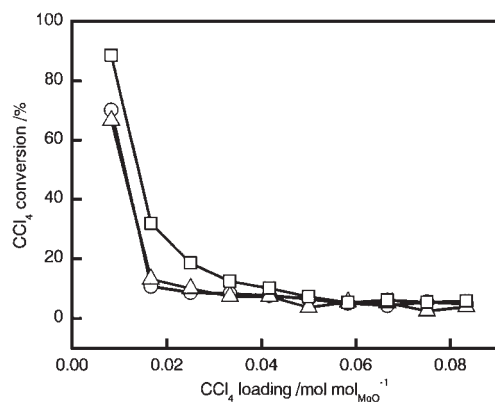


Fig. 11. CCl_4 decomposition by MgO (○), 5% $\text{MgF}_2\text{-MgO}$ (△), and 10% $\text{MgF}_2\text{-MgO}$ (□) at 723 K.

pulses of CCl_4 injection was observed, though at the first pulse of CCl_4 the conversion was as high as 89, 67, and 70% for 10% $\text{MgF}_2\text{-MgO}$, 5% $\text{MgF}_2\text{-MgO}$, and MgO , respectively. 10% $\text{MgF}_2\text{-MgO}$ with a high specific surface area of $233 \text{ m}^2 \text{ g}^{-1}$ showed slightly higher reactivity to CCl_4 than the other two. The ratio of surface-exposed MgO to MgO in the bulk was calculated to be 14.5%, based on the specific surface area and lattice constant of 4.21 \AA for MgO .³⁴ The final conversion of MgO calculated by the cumulative amount of CO_2 formed by 10 pulses of CCl_4 was about 3% showing that just one-fifth of surface-exposed MgO reacted with CCl_4 . It is also found by BET measurement and XRD analysis that, even with 1 pulse of CCl_4 , serious sintering of MgO crystallites occurred at the surface. From these results, we conclude that the acidity of MgO samples is not correlated to the reactivity to CCl_4 . Thus, most of the CCl_4 formed by CCl_2F_2 decomposition cannot be decomposed by partially fluorinated MgO , regardless of the degree of fluorination.

Weckhuysen et al. compared the reactivity of various alkaline earth metal oxides (MgO , CaO , SrO , and BaO) to CCl_4 and showed that the order in the reactivity to CCl_4 was as follows: $\text{BaO} > \text{SrO} > \text{CaO} > \text{MgO}$.¹⁰ This order is almost the same as that for the basicity and probably related to the size of the alkaline earth cation, while the acidity of the samples is quite important for the CCl_2F_2 decomposition in this study, as mentioned above. Decomposition of CCl_4 and CCl_2F_2 are clearly different in the reaction mechanism or the pathway to final products. Generally speaking, catalytic decomposition of CCl_2F_2 is more difficult than that of CCl_4 since C–F bonding is stronger than C–Cl bonding.^{2,5} Although the inclination seems to be in the opposite direction in decomposition with halogen fixation by MgO -based materials, dissociation of halogen–carbon bonding must be easier for CCl_4 than for CCl_2F_2 in the decomposition studied here. This can be seen in the experimental fact that initial CCl_4 conversion with MgO was high, as shown in Fig. 11 while for CCl_2F_2 decomposition at the same temperature of 723 K, MgO didn't show any reactivity at all (Fig. 4).

In this reaction, dissociation of halogen–carbon bonding is important for initiation of the reaction, however, the halogen fixation step (formation of halides) and the solid-state halogen exchange reaction to regenerate the reactive sites is rather important for continuous conversion. Absorption of chlorine as

MgCl_2 is clearly more difficult than absorption of fluorine which can proceed until conversion of MgO reaches about 90%. Thermodynamically favored formation of MgF_2 would be a reason for it. It can also be the reason that the solid-state ion exchange reaction between oxygen and chlorine is slower than that between oxygen and fluorine because the ion size of chloride is larger than that of fluoride (ion radii of O^{2-} , F^- , and Cl^- are 1.28, 1.18, and 1.67 \AA , respectively).

In the decomposition experiments of CCl_2F_2 at 623 K for $\text{MgF}_2\text{-MgO}$, the reactivity was greatly dependent on the degree of fluorination. The highest conversion of CCl_2F_2 during the reaction was obtained with 10% and 20% $\text{MgF}_2\text{-MgO}$, both of which have large specific acids. Thus, conversion should be related to the amount of acid sites. The induction period for CCl_2F_2 decomposition became shorter as the degree of fluorination became higher. 20% $\text{MgF}_2\text{-MgO}$ and 40% $\text{MgF}_2\text{-MgO}$ can be considered to have similar acid strengths according to $\text{NH}_3\text{-TPD}$ profiles (Fig. 6(d), (e)) and FT-IR analysis of pyridine adsorption. 20% $\text{MgF}_2\text{-MgO}$ has a larger amount of acid sites than 40% $\text{MgF}_2\text{-MgO}$, while the surface density of acid sites of 40% $\text{MgF}_2\text{-MgO}$ was larger than that of 20% $\text{MgF}_2\text{-MgO}$ (Table 2); hence, the induction period should be related to the surface density of acid sites when the strengths of acid sites of the samples are comparable. For initiation of CCl_2F_2 decomposition by $\text{MgF}_2\text{-MgO}$, strong Lewis acid sites with high density should be effective, since the CCl_2F_2 molecule has an electron distribution localized at the fluorine atoms due to its high electronegativity to have fluorine atoms somewhat negatively charged. Partially fluorinated magnesium oxides have the coordinatively unsaturated Mg sites with neighboring oxygen, which are generated by surrounding fluorides depending on the degree of fluorination. Because the coordinatively unsaturated Mg sites behave as Lewis acids, $\text{MgF}_2\text{-MgO}$ with high degree of fluorination reacts with CCl_2F_2 more easily than those with lower degrees of fluorination. From a mechanistic point of view, the first step of CCl_2F_2 decomposition will be dissociative chemisorption of fluorine to form CCl_2 from CCl_2F_2 on the Lewis acid sites. Then extraction of O^{2-} ion from the MgO lattice occurs in succession to form phosgene, followed by conversion of COCl_2 to CCl_4 and CO_2 via two ways: the one is a disproportionation of COCl_2 , the other is the dissociative chemisorption of COCl_2 onto MgO to form CO_2 and magnesium chloride, and then halogen exchange between MgCl_2 and CCl_2F_2 takes place to form CCl_4 and MgF_2 . Formed CCl_4 are not decomposed downstream due to the low reactivity of $\text{MgF}_2\text{-MgO}$ to CCl_4 as mentioned above. As shown in Table 4, by procession of the reaction, the surface density of fluoride becomes higher to create stronger Lewis acid sites with higher surface density. Conversion of CCl_2F_2 diminished as the amount of acidic Mg sites with neighboring oxygen decreased. In this way, selective fluorine absorption takes place accompanied by formation of CCl_4 and CO_2 in equimolar amounts by $\text{MgF}_2\text{-MgO}$ with moderately dense and strong Lewis acid sites.

As the other byproduct, a small amount of CCl_3F was observed, as shown in Fig. 8. In this case, formation of CCl_3F became maximum around 80% of MgF_2 content. Moreover, obvious CCl_3F formation was observed under circumstances that showed the difficulty in C–F bond dissociation: CCl_2F_2 decom-

position by 10% MgF₂-MgO at 573 K and CCl₂F₂ decomposition by 5% MgF₂-MgO at 623 K. Those conditions of low reaction temperature and weak acidity of the sample would cause incomplete dissociation of C-F bonds to form CCl₂F intermediates, which would combine with Cl to form CCl₃F. In general, decomposition of CCl₃F is easier than that of CCl₂F₂ due to lower binding energy of both C-Cl and C-F bonding; then further halogen exchange to form CCl₄ would easily occur. This would be the reason for small amount of CCl₃F formation and exclusive formation of CCl₄ as final product, if there are sufficient active sites. The equation for selective fluorine adsorption and formation of CCl₃F can be described as Eq. 3. The lack of CClF₃ as a product definitely shows that disproportionation of CCl₂F₂ to form CCl₃F and CClF₃ does not occur.



$$\Delta H^0 = -532 \text{ kJ mol}^{-1}. \quad (3)$$

The mechanism of CCl₂F₂ decomposition and the pathway for product formation should become independent of reaction temperature between 623 and 773 K and the degree of fluorination higher than 5%, since in all such cases the reactivity to CCl₄ was quite low. Decomposition of CCl₄ and fixation of chlorine can be attained by using other alkaline earth metal oxides such as CaO, SrO, or BaO. Thus, formation of CCl₄ as product is not a crucial problem for practical application of this method. Combination of the systems using partially fluorinated MgO and using other alkaline earth metal oxides can allow both chlorine and fluorine of CCl₂F₂ to be separately fixed.

Conclusions

Partially fluorinated magnesium oxides (MgF₂-MgO) were found to be highly reactive in CCl₂F₂ decomposition with selective fluorine absorption as MgF₂. The reactivity was related to the degree of fluorination of MgO. The amount and strength of acid sites on MgF₂-MgO analyzed by NH₃-TPD drastically changed depending on the degree of fluorination. Pyridine adsorption experiments using FT-IR to characterize acid sites for MgO and partially fluorinated MgO indicated that partially fluorinated MgO had Lewis acid sites and no Brønsted acid sites. By increasing the degree of fluorination, Lewis acidity became slightly stronger, as suggested by slight shift in the absorption bands by ring vibration modes 8a and 19b of pyridine. Thus, the initial stage of CCl₂F₂ decomposition was considered to occur on Lewis acid sites to dissociate C-F bonds. Mg-F bonding was subsequently formed after the dissociation of C-F in CCl₂F₂ and highly electronegative fluorine atoms generated coordinatively unsaturated Mg sites at their surroundings. As a result, Lewis acid sites are also generated by partially fluorination of MgO by CCl₂F₂, so CCl₂F₂ decomposition with fluorine fixation proceeds at high efficiency. CCl₄ decomposition by MgO and partially fluorinated MgO proceeded very slowly. This low reactivity to CCl₄ was considered to be a dominant factor for selective MgF₂ formation in CCl₂F₂ decomposition by MgO and MgF₂-MgO.

References

1 Y. Takita, G.-R. Li, R. Matsuzaki, H. Wakamatsu, H. Nishiguchi, Y. Moro-oka, and T. Ishihara, *Chem. Lett.*, **1997**, 13.

2 Y. Takita, H. Wakamatsu, M. Tokumaru, H. Nishiguchi, M. Ito, and T. Ishihara, *Appl. Catal., A*, **194**, 55 (2000).

3 Y. Takita, M. Ninomiya, R. Matsuzaki, H. Wakamatsu, H. Nishiguchi, and T. Ishihara, *Phys. Chem. Chem. Phys.*, **1**, 2367 (1999).

4 X. Deng, Z. Ma, Y. Yue, and Z. GaO, *J. Catal.*, **204**, 200 (2001).

5 M. Tajima, M. Niwa, Y. Fujii, Y. Koinuma, R. Aizawa, S. Kushiyama, S. Kobayashi, K. Mizuno, and H. Ohuchi, *Appl. Catal., B*, **9**, 167 (1996).

6 S. Karmakar and H. L. Greene, *J. Catal.*, **151**, 394 (1995).

7 S. Karmakar and H. L. Greene, *J. Catal.*, **148**, 524 (1994).

8 X. Fu, W. A. Zeltner, Q. Yang, and M. A. Anderson, *J. Catal.*, **168**, 482 (1997).

9 B. M. Weckhuysen, M. P. Rosynek, and J. H. Lunsford, *Phys. Chem. Chem. Phys.*, **1**, 3157 (1999).

10 B. M. Weckhuysen, G. Mestl, M. P. Rosynek, T. R. Klawietz, J. F. Haw, and J. H. Lunsford, *J. Phys. Chem. B*, **102**, 3773 (1998).

11 K. J. Klabunde, J. Stark, O. Koper, C. Mohs, D. G. Park, S. Decker, Y. Jiang, I. Lagadic, and D. Zhang, *J. Phys. Chem.*, **100**, 12142 (1996).

12 Y. Jiang, S. Decker, C. Mohs, and K. J. Klabunde, *J. Catal.*, **180**, 24 (1998).

13 K. J. Klabunde, A. Khaleel, and D. Park, *High Temp. Mater. Sci.*, **33**, 99 (1995).

14 S. P. Decker, J. S. Klabunde, A. Khaleel, and K. J. Klabunde, *Environ. Sci. Technol.*, **36**, 762 (2002).

15 O. Koper, I. Lagadic, and K. J. Klabunde, *Chem. Mater.*, **9**, 838 (1997).

16 O. Koper, E. A. Wovchko, J. A. Glass, J. T. Yates, and K. J. Klabunde, *Langmuir*, **11**, 2054 (1995).

17 J. Burdenic and R. H. Crabtree, *Science*, **27**, 340 (1996).

18 M. C. Lee and W. Choi, *Environ. Sci. Technol.*, **36**, 1367 (2002).

19 D. P. Dufaux and M. R. Zachariah, *Environ. Sci. Technol.*, **3**, 2223 (1997).

20 T. Tamai, K. Inazu, and K. Aika, *Chem. Lett.*, **32**, 436 (2003).

21 A. Hess and E. Kemnitz, *J. Catal.*, **149**, 449 (1994).

22 A. Alonso, A. Morato, F. Medina, Y. Cesteros, P. Salagre, and J. E. Sueiras, *Appl. Catal., B*, **40**, 259 (2003).

23 A. Hess, E. Kemnitz, A. Lippitz, W. E. S. Unger, and D. H. Menz, *J. Catal.*, **148**, 270 (1994).

24 M. Shimbo, Z. Nakagawa, Y. Ohya, and K. Hamano, *J. Ceram. Soc. Jpn.*, **97**, 640 (1989).

25 H. Itoh, S. Utanapanya, J. V. Stark, K. J. Klabunde, and J. R. Shulup, *Chem. Mater.*, **5**, 71 (1993).

26 T. López and R. Gómez, *J. Sol-Gel Sci. Technol.*, **13**, 1043 (1998).

27 A. H. Kline and J. Turkevich, *J. Chem. Phys.*, **12**, 300 (1944).

28 G. Connell and J. A. Dumesic, *J. Catal.*, **101**, 103 (1986).

29 H. Noller, J. A. Lercher, and H. Vinex, *Mater. Chem. Phys.*, **18**, 577 (1998).

30 J. W. Wald, *J. Catal.*, **10**, 34 (1968).

31 S. Okazaki, *Shokubai*, **10**, 242 (1968).

32 E. Kemnitz, Y. Zhu, and B. Adamczyk, *J. Fluorine Chem.*, **114**, 163 (2002).

33 M. Wojciechowska, M. Zielinski, and M. Pietrowski, *J. Fluorine Chem.*, **120**, 1 (2003).

34 Y.-X. Li and K. J. Klabunde, *Langmuir*, **7**, 1388 (1991).